Biomarker-based assessment of sublethal toxicity of organic UV filters (ensulizole and octocrylene) in a sentinel marine bivalve *Mytilus edulis*

Halina Falfushynska [a,b], Eugene P. Sokolov [c], Kathrin Fisch [d], Hatem Gazie [d], Detlef E. Schulz-Bull [d], Inna M. Sokolova [a,e,*]

[a] *Department of Marine Biology, Institute for Biological Sciences, University of Rostock, Rostock, Germany*
[b] *Department of Human Health, Physical Rehabilitation and Vital Activity, Ternopil V. Hnatiuk National Pedagogical University, Ternopil, Ukraine*
[c] *Leibniz Institute for Baltic Sea Research, Leibniz Science Campus Phosphorus Research, Warnemünde, Rostock, Germany*
[d] *Department Marine Chemistry, Leibniz-Institute for Baltic Sea Research Warnemünde, Seestr. 15, 18119 Rostock, Germany*
[e] *Department of Maritime Systems, Interdisciplinary Faculty, University of Rostock, Rostock, Germany*

HIGHLIGHTS

- Toxicological investigation of two UV filters at environmentally relevant concentrations.
- Ensulizole and octocrylene cause sublethal effects in mussels.
- Octocrylene-induced stress is concentration dependent.
- Ensulizole is more toxic at lower concentration levels.

GRAPHICAL ABSTRACT
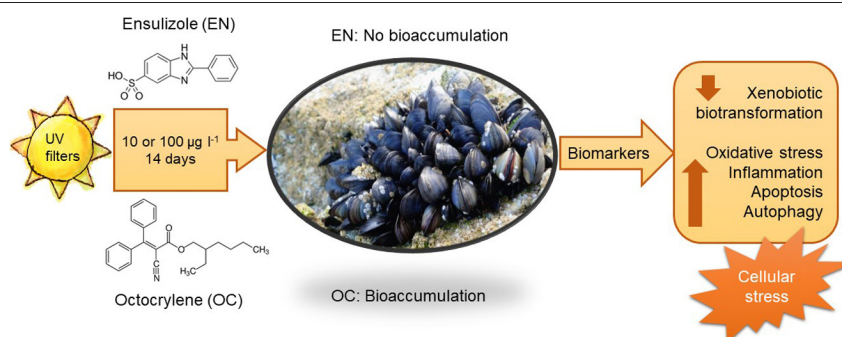
ARTICLE INFO

ABSTRACT

The global occurrence of organic UV filters in the marine environment is of increasing ecotoxicological concern. Here we assessed the toxicity of UV filters ensulizole and octocrylene in the blue mussels *Mytilus edulis* exposed to 10 or 100 μg l^{-1} of octocrylene and ensulizole for two weeks. An integrated battery of biochemical and molecular biomarkers related to xenobiotics metabolism and cellular toxicity (including oxidative stress, DNA damage, apoptosis, autophagy and inflammation) was used to assess the toxicity of these UV filters in the mussels. Octocrylene (but not ensulizole) accumulated in the mussel tissues during the waterborne exposures. Both studied UV filters induced sublethal toxic effects in *M. edulis* at the investigated concentrations. These effects involved induction of oxidative stress, genotoxicity (indicated by upregulation of DNA damage sensing and repair markers), upregulation of apoptosis and inflammation, and dysregulation of the xenobiotic biotransformation system. Octocrylene induced cellular stress in a concentration-dependent manner, whereas ensulizole appeared to be more toxic at the lower (10 μg l^{-1}) studied concentration than at 100 μg l^{-1}. The different concentration-dependence of sublethal effects and distinct toxicological profiles of ensulizole and octocrylene show that the environmental toxicity is not directly related to lipophilicity and bioaccumulation potential of these UV filters and demonstrate the importance of using bioassays for toxicity assessment of emerging pollutants in coastal marine ecosystems.

© 2021 Published by Elsevier B.V.

* Corresponding author at: Department of Marine Biology, Institute for Biological Sciences, University of Rostock, Rostock, Germany.
 E-mail address: inna.sokolova@uni-rostock.de (I.M. Sokolova).

1. Introduction

Estuaries and coastal areas are highly productive yet vulnerable aquatic ecosystems exposed to high anthropogenic pressure. Increasing coastal urbanization and tourism result in high influx of human-associated pollutants including pharmaceuticals and personal care products (PPCPs) such as sunscreens into the estuarine and coastal waters (Sánchez-Quiles and Tovar-Sánchez, 2015). The organic and inorganic ultraviolet (UV) filters from sunscreens reach the marine environment both directly as a consequence of the recreational activities and/or indirectly from wastewater treatment plants (WWTP) effluents (Fisch et al., 2021; Sánchez-Quiles and Tovar-Sánchez, 2015). UV filters from sunscreens are found in a variety of environmental matrices including wastewaters, freshwater bodies, soil, coastal surface waters, sediments and biota (Bachelot et al., 2012; Balázs et al., 2016; Fisch et al., 2017; Pintado-Herrera and Lara Martín, 2020; Sánchez-Quiles and Tovar-Sánchez, 2015). In coastal marine waters, the UV filters' concentrations fluctuate from low ng l^{-1} to dozens of µg l^{-1}, depending on the location, season and time of the day (Blasco et al., 2020). Organic UV filters can accumulate in marine organisms reaching levels from a few µg kg^{-1} to >10 mg kg^{-1} body mass (Lozano et al., 2020). However, the implications of the sunscreens as a potential environmental hazard have been poorly evaluated in the estuarine and coastal marine systems (Pintado-Herrera and Lara Martín, 2020; Sánchez-Quiles and Tovar-Sánchez, 2015).

Sunscreens represent a complex mixture of inorganic (mostly nano-ZnO and nano-TiO$_2$) and organic UV filters that reflect, absorb or scatter the UV radiation (Gilbert et al., 2013; Sánchez-Quiles and Tovar-Sánchez, 2015). Recent studies [reviewed in (Gilbert et al., 2013; Luo et al., 2020; Yung et al., 2015)] demonstrate considerable toxicity of nano-ZnO and nano-TiO$_2$ to marine biota and high ecosystem risk due to their accumulation in the coastal waters and sediment (Luo et al., 2020; Minetto et al., 2016; Scown et al., 2010). In contrast, the ecotoxicity of organic UV filters remains little explored in marine organisms. Recent studies show that organic UV filters can disturb embryonic and larval development and cause neurotoxicity in marine organisms (Lozano et al., 2020). Recently, two US states (Hawaii and Florida), as well as Mexico and Palau have banned certain organic UV filters (such as oxybenzone and octinoxate) due to the negative impacts on the coral development and bleaching (Downs et al., 2016; He et al., 2019; Schneider and Lim, 2019). However, the environmental risks of UV filters remain controversial due to insufficient research in this field (Corinaldesi et al., 2018; Fel et al., 2019; He et al., 2019), particularly with regard to the potential sublethal effects of environmentally relevant concentrations of organic UV filters (Lozano et al., 2020). Furthermore, many recent studies on sunscreen toxicity focused on the tropical (coral reef) ecosystems (Corinaldesi et al., 2018; Downs et al., 2016; Fel et al., 2019; He et al., 2019), while the impacts of the UV filters on temperate marine organisms remain poorly understood.

In this study, we focused on a multi-biomarker based assessment of toxicity of two common UV filters, ensulizole (phenylbenzimidazole sulfonic acid) and octocrylene (2-ethylhexyl 2-cyano-3,3-diphenyl-2-propenoate) broadly used in sunscreen formulations (Cosing database http://data.europa.eu, accessed on 14.04.21). Due to their poor removal by the WWTPs as well as the direct input into the water through recreational activities, these compounds are ubiquitously found in the surface water and sediments (Apel et al., 2018; Fisch et al., 2021; Mitchelmore et al., 2019; Sánchez-Quiles and Tovar-Sánchez, 2015; Sang and Leung, 2016; Tsui et al., 2015) including the Baltic Sea (Fisch et al., 2017). The levels of ensulizole and octocrylene range from ng l^{-1} to µg l^{-1} in surface waters and µg kg^{-1} in sediment (Fisch et al., 2017; Grabicova et al., 2013; Apel et al., 2018). Octocrylene is a lipophilic compound that strongly accumulates in aquatic organisms (Kaiser et al., 2012; Lozano et al., 2020) and can cause toxic effects including neurotoxicity (Ruszkiewicz et al., 2017), endocrine disruption (Yan et al., 2020; Zhang et al., 2016), developmental toxicity (Blüthgen

et al., 2014; Yan et al., 2020), bioenergetic disturbances (Stien et al., 2019) and interference with lipid metabolism (Stien et al., 2019). Ensulizole is hydrophilic and has lower capacity to bioaccumulate than octocrylene (European Chemicals Agency https://echa.europa.eu/de/information-on-chemicals, accessed on 14.04.21), and its toxic effects in aquatic organisms are not known.

We used the blue mussel *Mytilus edulis* as a model species to assess the toxic mechanisms of ensulizole and octocrylene in marine organisms. *M. edulis* is a common sentinel species for ecotoxicological assessments due to its well understood physiology, broad geographical distribution and ability to accumulate pollutants. Because the toxic mechanisms of UV filters are poorly understood, we used a broad battery of biomarkers focusing on the putative toxicity pathways that commonly respond to organic contaminants including oxidative stress (generation of reactive oxygen species (ROS), oxidative lesions to lipids and proteins, and activity of a key antioxidant enzyme glutathione reductase), general cellular stress response (lysosomal membrane stability and activity of an autophagic marker enzyme, cathepsin D) and xenobiotic biotransformation system capacity (measured by the activities of NADPH-cytochrome P450-oxidoreductase, CYP450 1A monooxygenase, carboxylesterase and glutathione S-transferase) in the mussels exposed for two weeks to 10 and 100 µg l^{-1} of ensulizole and octocrylene in seawater. Furthermore, the potential role of apoptosis, inflammation, DNA damage and lipid metabolism disruption in the sublethal toxicity of octocrylene and ensulizole was tested by assessing mRNA expression of the key marker genes involved in the respective pathways including caspases 2 and 3, BAX and Bcl-2 (for apoptosis), NF-κB and interleukin IL-17 (for inflammation), the Guardian of the Genome tumor protein p53 and the growth arrest and DNA-damage-inducible protein GADD45 (for genotoxicity) and acetyl-CoA carboxylase ACC, the peroxisome proliferator-activated receptor PPARγ and cyclooxygenase 2 COX-2 (for lipid metabolism). Our study demonstrated distinct toxicological profiles of the two studied UV filters in the mussels and showed that environmental toxicity of the two studied UV filters is not directly related to their lipophilicity and bioaccumulation potential.

2. Materials and methods

2.1. Chemicals

All chemicals were purchased from Sigma Aldrich/Merck (Germany), Carl Roth (Germany), and VWR (Germany) and were of the analytical grade or higher. For experimental exposures, certified reference materials of octocrylene (Supelco Analytical, catalog # PHR1083) and ensulizole (Sigma Aldrich, catalog # 437166) were purchased from Merck (Germany). The internal standard benzophenone-3-d5 (BP-3-d5) was purchased from CDN Isotopes (Canada).

2.2. Experimental exposures

Adult mussels (mean shell length 42.6 ± 0.9 mm, wet tissue mass 4.15 ± 0.25 g, $N = 60$) were collected near Warnemünde, Germany (54°10′49.602″N, 12°05′21.991″E). The studied population represents *Mytilus edulis* × *M. trossulus* hybrids with predominant genetic background of *M. edulis* (Stuckas et al., 2017); therefore, the experimental animals were designated *M. edulis*. The mussels were transported to the University of Rostock in a humid cooler within 2 h of collection, surface-cleaned and kept in aerated, temperature-controlled aquaria with a protein skimmer and a moving bed biofilter. The mussels were acclimated at 15 ± 1 °C and salinity 15 ± 1 for two weeks prior to the experiments. These conditions were close to the habitat salinity and temperature at the time of collection.

After the preliminary acclimation, mussels were randomly assigned to one of the following five groups: 1) control (no organic UV filters addition, 0.0001% v/v dimethyl sulfoxide (DMSO) as vehicle control); 2) 10 µg l^{-1} of ensulizole (EN10); 3) 100 µg l^{-1} of ensulizole (EN100);

4) 10 µg l^{-1} of octocrylene (OC10); 5) 100 µg l^{-1} of octocrylene (OC100). Stock solutions of octocrylene were prepared in DMSO, and the final concentration of DMSO in all octocrylene exposures was 0.0001%. Pilot studies showed that 0.0001% DMSO has no effect on any of the studied biomarkers in *M. edulis* (data not shown). The stock solutions of ensulizole were made with water. The lower concentrations of studied organic filters (10 µg l^{-1}) were within the range of the concentrations reported in the environmental samples (Fisch et al., 2017; Grabicova et al., 2013; Langford and Thomas, 2008; O'Malley et al., 2019; Rodil and Moeder, 2008). A higher concentration (100 µg l^{-1}) was included for hazard assessment and elucidation of the potential toxic mechanisms of the studied UV filters.

Randomized block design was used for experimental exposures with two tanks per treatment, each containing 15 mussels in 5 l of artificial seawater (Instant Ocean® Sea Salt) at 15 ± 1 °C, salinity 15 ± 1 and 12:12 light: dark regime. To maintain the water quality and target concentrations of the UV filters, the water was changed and chemicals were added twice a week. Preliminary testing showed that ensulizole and octocrylene solutions in seawater (in the absence of animals) were stable for at least 7 days (longer times were not tested). Water samples were collected from the tanks 2 h before the water change and shortly after the water change to measure ensulizole and octocrylene concentrations. Ammonia and nitrites levels in the exposure tanks were controlled by common analytical protocols and did not exceed permitted values for salt water. During the preliminary acclimation and experimental exposures, mussels were fed ad libitum 2 h before the water change with a commercial blend of live algae containing *Nannochloropsis oculata*, *Phaeodactylum* sp. and *Chlorella* sp. (Premium Reef Blend, CoralSands, Wiesbaden, Germany) per manufacturer's instructions. No mortality of the mussels occurred during the experimental exposures. Mussels were exposed to the organic UV filters for 14 days. Two weeks is considered sufficient time to achieve acclimation (marked by physiological steady-state) after an environmental shift in temperate marine bivalves (Khlebovich, 2017).

After 14 days of exposure, mussels were dissected on ice, and hemolymph, gills and digestive gland tissues were collected. Lysosomal membrane stability and reactive oxygen species (ROS) production were determined in the hemocytes, and biochemical markers (including oxidative lesions and enzyme activities) were measured in the digestive gland and the gills. The mRNA expression of molecular markers (including those related to apoptosis, inflammation, DNA damage and repair, and lipid metabolism) were assessed in the digestive gland. The gills are the main gas and ion exchange organs of the mussels and a major uptake site for the waterborne pollutants (Gosling, 2003), whereas the digestive gland is a key organ for pollutant accumulation and detoxification (Faggio et al., 2018). Hemocytes were studied immediately, while the digestive gland and gill samples were shock-frozen in liquid nitrogen and stored at −80 °C until further analyses. A pilot analysis detected no significant effects of experimental tanks on the studied traits ($P > 0.05$). Therefore, individual mussels ($N = 6$ per treatment) were considered biological replicates in subsequent analyses.

2.3. UV filter analyses in water and mussel tissues

Water samples (1 ml for EN10, EN100 and OC100, and 4 ml for OC10) were enriched and cleaned-up via solid phase extraction prior the LC-MS/MS analysis. The OASIS HLB (6 cc, 500 mg, Waters) cartridges were pre-conditioned with 4 ml methanol and 4 ml water (LC-grade). The samples were acidified with 5 M HCl to pH 3 and spiked with an internal standard (BP-3-d5). After extraction the cartridges were cleaned with 4 ml water (pH 3) and dried under a stream of nitrogen. The cartridges were eluted with 4 ml acetone:methanol (1:1, *v/v*) and 6 ml methanol. The eluate was evaporated at 42 °C in clean air (2–3 bar) using a sample concentrator (Stuart™, UK). The samples were reconstituted in 1 ml water for ensulizole or 1 ml water:methanol (1:1, *v/v*) for octocrylene, and

transferred into amber vials via a syringe filter (0.45 µm, Phenomenex, Germany).

The mussel tissues collected after 14 days of exposure were combined within each experimental exposure group (controls, EN10, EN100 and OC100) due to limited sample material. This resulted in a single sample per treatment, each consisting of tissues of 15 mussels. Samples from the OC10 groups were excluded from this analysis, since the octocrylene levels in the exposure water were below the limit of detection. All samples were freeze dried and homogenized. For each sample, up to 1 g of dry tissue mass was spiked with 20 ng ml^{-1} of BP-3-d5 and deuterated octocrylene (OC-d15). The samples were extracted with three different solvents: 1) 4 ml water:methanol (1:1, *v/v*) 2) 4 ml methanol, and 3) 4 ml acetonitrile. Extracts were ultrasonicated for 10 min at 22 °C and centrifuged for 10 min at 4000 xg. Supernatants from extractions with different solvents were combined and processed as described above for the eluted water samples.

Samples were analyzed with the LC-MS/MS method according to Fisch et al., 2021, with a slight modification of the gradient program: 0.5 min A (75%) and B (25%), 4 min A (10%) and B (90%), kept for 5 min, 9.5 min A (75%) and B (25%) kept for 1.5 min (A: water +0.1% acetic acid, B: methanol +0.1% formic acid). For quality and quantity assurance standards (10 and 100 ng ml^{-1}) were measured with the samples. The concentrations were determined based on the calibrations curves in the range 1–150 ng ml^{-1} ($N = 10$) and the recovery rates (EN10: 30%, EN100: 86%, OC10: 50%, OC100: 50%).

2.4. Lysosomal membrane integrity and ROS generation in hemocytes

Hemolymph was withdrawn from the adductor muscle of the mussels. Hemocytes were pelleted at 500 $\times g$, washed using a hemocyte buffer containing 20 mmol L^{-1} 4-(2-hydroxyethyl)-1-piperazineethanesulfonic acid (HEPES), 436 mmol L^{-1} NaCl, 53 mmol L^{-1} MgSO$_4$, 10 mmol L^{-1} CaCl$_2$ and 10 mmol l^{-1} KCl, pH 7.3, and counted using BrightLine hemacytometer. The hemocytes (1×10^7 cells ml^{-1}) were resuspended in the hemocyte buffer. Lysosomal membrane integrity was determined in hemocyte suspension by the Neutral Red Retention (NRR) assay as described elsewhere (Repetto et al., 2008).

ROS generation was determined by reduction of nitroblue tetrazolium (NBT) dye by superoxide (Muñoz et al., 2000). The hemocytes were incubated for 2 h in the buffer containing 20 mmol l^{-1} HEPES, 436 mmol l^{-1} NaCl, 53 mmol l^{-1} MgSO$_4$, 10 mmol l^{-1} CaCl$_2$ and 10 mmol l^{-1} KCl, pH 7.3, 10 µg ml^{-1} phorbol-12-myristat-13-acetate (to stimulate ROS production) and 0.3% NBT. After the incubation, the hemocytes were fixed in absolute methanol. The formazan deposits were solubilized in 2 M KOH: dimethyl sulfoxide (DMSO) (5:6 *v/v*), and the absorbance was read at 620 nm using a SpectraMax M2 microplate reader (Molecular Devices GmbH, Biberach-an-der-Riß, Germany) with LightPath correction.

2.5. Oxidative stress markers

Lipid peroxidation (LPO) was determined in homogenates of the digestive gland and gills by the formation of the thiobarbituric acid-reactive substances (TBARS) (Ohkawa et al., 1979). Protein carbonyl (PC) concentrations were measured in the digestive gland and gills based on the reaction of the carbonyl groups with 2,4-dinitrophenylhydrazine (DNPH) (Reznick and Packer, 1994). The absorbance was determined at 532 nm (TBARS) or 370 nm (carbonyls) using a SpectraMax M2 microplate reader with LightPath correction (Molecular Devices GmbH, Biberach-an-der-Riß, Germany). Molar extinction coefficients of $1.56 \cdot 10^5$ M^{-1} cm^{-1} and $2.2 \cdot 10^4$ M^{-1} cm^{-1} were used to calculate TBARS and PC concentrations, respectively.

2.6. Activities of biotransformation and antioxidant enzymes

All enzymatic assays were conducted in the digestive gland and gill tissues using standard assay protocols described elsewhere

(Falfushynska et al., 2019). NADPH–P450 reductase (CPR) and 7-ethoxyresorufin-O-deethylase (EROD) activities were determined in the microsomal fractions of the digestive gland and gills. Microsomal fractions were isolated by differential centrifugation of tissue homogenates (1:4 w/v) in 10 mM Tris-sucrose buffer (Balk et al., 1982). The post-mitochondrial supernatants were centrifuged for 1 h at 100,000 $\times g$, and the microsome-containing pellet was resuspended in the buffer containing 100 mM Tris pH 7.6, 1 mM ethylenediaminetetraacetic acid (EDTA), and 20% (v/v) glycerol. The CPR activity was measured as the NADPH-dependent reduction of cytochrome c (Guengerich et al., 2009). EROD activity was assessed by the rate of the CYP1A-mediated deethylation of 7-ethoxyresorufin (Mohammadi Bardbori, 2014).

Carboxylesterase (CE) activity was determined in the soluble protein fraction of the tissue homogenates by the rate of hydrolysis of *p*-nitrophenyl acetate (Hosokawa and Satoh, 2002). The formation of ρ-nitrophenol was registered at 405 nm, and the enzyme activity was calculated using the extinction coefficient of 18 mM^{-1} cm^{-1}. Glutathione S-transferase (GST) activity was measured in the digestive gland and gill tissue homogenates using 1-chloro-2,4-dinitrobenzene (CDNB) reduction assay (Habig et al., 1974). GST activity was determined from the rate of change in CDNB absorbance at 340 nm using the extinction coefficient of 9.6 mM^{-1} cm^{-1}. The catalytic activity of glutathione reductase (GR) was determined spectrophotometrically by conversion of oxidized to reduced glutathione in the presence of NADPH (Carlberg and Mannervik, 1975).

2.7. Quantitative RT-PCR

Total RNA was extracted from the digestive gland tissue using TRI Reagent® (Sigma, St. Louis, MO) and cleaned from possible DNA contamination using TURBO DNA-free Kit (Thermo Fisher Scientific, Berlin, Germany) according to the manufacturers' instructions. cDNA was obtained from 2 μg of the total RNA using High Capacity cDNA Reverse Transcription Kit (Thermo Fisher Scientific, Berlin, Germany). Quantitative PCR was carried out using StepOnePlus™ Real-Time PCR System Thermal Cycling Block (Applied Biosystems, Thermo Fisher Scientific, Berlin, Germany) and Biozym Blue S'Green qPCR Mix Separate ROX kit (Biozym Scientific GmbH, Hessisch Oldendorf, Germany) as described earlier (Steffen et al., 2020). Depending on the published sequence availability, we used sequences from *M. edulis* or a closely related species *Mytilus galloprovincialis* that belongs to *M. edulis* species complex (Gaitán-Espitia et al., 2016; Varvio et al., 1988) for primer design (Table 1). For IL-17, published primers for *Mytilus corsucus* were used (Qi et al., 2019). In each run, serial dilutions of a cDNA standard were amplified to determine the apparent amplification efficiency (Pfaffl, 2001), and a melt curve analysis was performed to ensure that a single PCR product was amplified. The expression of the target genes was normalized against the expression of eukaryotic elongation factor eEF1 (Pfaffl, 2001; Steffen et al., 2020).

2.8. Data analyses

The normality and homogeneity of variances were checked using Kolmogorov-Smirnov and Levine tests, respectively. If the data didn't meet the requirements of normality or homogeneity of variances, Box-Cox or log$_{10}$ transformation was used. The effects of experimental exposure on the biological traits were tested using one-way ANOVA. Fisher's Least Significant Difference (LSD) test was used to determine which pairs of means are significantly different from each other.

Normalized data were subjected to the principal component analysis (PCA) to identify the patterns of responses of the biochemical and physiological biomarkers to the effects of octocrylene and ensulizole and compare these patterns in different experimental groups. Discriminant function analysis was used to determine which variables are important to distinguish the experimental groups of mussels depending on the substance and its concentration. All statistical calculations were performed with Statistica v. 12.0 and Excel for Windows-2016. Differences were considered significant if the probability of Type I error was <0.05. All data are reported as the mean ± the standard error unless indicated otherwise.

3. Results

3.1. UV filter levels in experimental exposures

Concentrations of ensulizole measured in the water were close to the nominal concentrations and did not change considerably during the mussels' exposure. Thus, the measured ensulizole concentrations in the 10 μg l^{-1} exposure were (mean ± S.D.): 9.83 ± 1.18 μg l^{-1} and 11.33 ± 1.12 μg l^{-1} shortly after the water change and before the next water change, respectively ($N = 6$). In the high (100 μg l^{-1}) ensulizole exposures, the measured water concentrations were 110.54 ± 13.12 μg l^{-1} and 109.62 ± 12.11 μg l^{-1} shortly after the water change and before the next change, respectively (N = 6). Dissolved octocrylene concentrations were lower than the nominal concentrations, and were below the detection limit in the low (10 μg l^{-1}) exposures and ranged from 16.2 ± 13.12 μg l^{-1} (shortly after the water change) to 1.4 ± 0.3 μg l^{-1} (before the water change) in the 100 μg l^{-1} exposure (N = 6). No ensulizole was detected in the mussels' tissues in this study, whereas mussels exposed to octocrylene accumulated ~104 ng g^{-1} dry mass of octocrylene ($N = 1$ using a combined sample of 15 mussels after 14 days of exposure).

3.2. General stress indices in hemocytes

Neutral red retention (NRR) (an index of the lysosomal membrane integrity) decreased in the concentration-dependent manner in the hemocytes of the mussels exposed to 10 and 100 μg l^{-1} ensulizole or octocrylene (Fig. 1A). Exposure to 10 μg l^{-1} ensulizole stimulated

Table 1
Primer sequences for the target and housekeeping genes used for mRNA analyses in *M. edulis* digestive gland.

Gene	Forward primer (5′-3′)	Reverse primer (5′-3′)	Reference or NCBI accession #
Caspase 2	ACAAGTGCAGATGCTGTGTTG	ACACCTCTCACATTGTCGGC	HQ424449
Caspase 3	ACGACAGCTAGTTCACCAGG	CCACCAGAAGAGGAGTTCCG	HQ424453
Bcl-2	CGGTGGTTGGCAAGGATTTG	CGCCATTGCGCCTATTACAC	KC545829
BAX	TAACTGGGGACGTGTAGGCA	CCAGGGGGCGACATAATCTG	KC545830
NF-κB	TGGATGATGAGGCCAAACCC	TGAAGTCCACCATGTGACGG	KF051275
ACC	GGTCATCTGTGGGGCATTAC	ACATCCACCTTGTTGTTCAGG	JX273654
IL-17	GGAGTTTGCGAAAATGGCGT	AGCACCGATTGGAGGACTTG	(Qi et al., 2019)
p53	AAGCTGGCTCAGAATGGGTC	TTCGACTGCCCGTCTACCTA	AY579472
GADD45	GCACAGGAAGACGGCAGAATT	TCTGTTTCGGCCATCTCTGGT	AJ623737
COX-2	CATTAGTCAAGAACGAAAGTCAGAG	GCCTGCCGAGTCATTGAAG	FJ490762
EF1	GACAGCAAAAACGACCCACC	TTCTCCAGGGTGGTTCAGGA	AF063420

Gene abbreviations: Bcl-2 - B-cell lymphoma 2; BAX - Bcl-2-associated X protein; NF-κB – nuclear factor κB; ACC - acetyl-CoA carboxylase; IL-17 – interleukin 17, p53 – tumor protein 53; GADD45 - growth arrest and DNA-damage-inducible protein 45; COX-2 – cyclooxygenase 2; EF1 – eukaryotic elongation factor 1α.
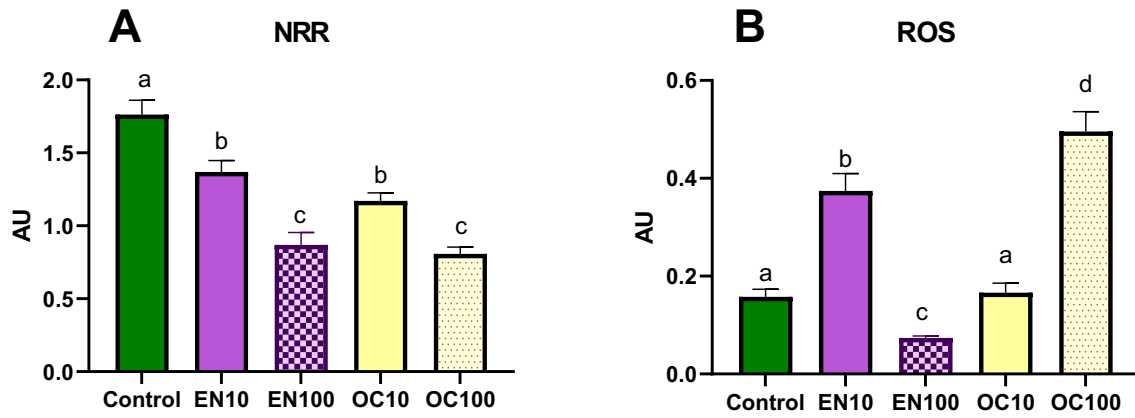
Fig. 1. Effects of ensulizole (EN) and octocrylene (OC) exposures on neutral red retention (NRR) and ROS production in the hemocytes of *M. edulis*. Mussels were exposed for two weeks to $10\ \mu g\ l^{-1}$ (EN10, OC10) or $100\ \mu g\ l^{-1}$ (EN100, OC100) of the respective UV filters. Columns that do not share letters represent significantly different values ($P < 0.05$). (For interpretation of the references to colour in this figure legend, the reader is referred to the web version of this article.)

ROS production in the mussel hemocytes; this effect was reversed at $100\ \mu g\ l^{-1}$ ensulizole (Fig. 1B). Exposure to low ($10\ \mu g\ l^{-1}$) concentrations of octocrylene had no effect on the hemocyte ROS production, whereas high levels ($100\ \mu g\ l^{-1}$) strongly stimulated ROS production (Fig. 1B).

3.3. Oxidative stress

Levels of the lipid peroxidation markers (TBARS) increased in response to the ensulizole exposures (at $10\ \mu g\ l^{-1}$ in the digestive gland and at both studied concentrations in the gills) (Fig. 2A, B). Exposures
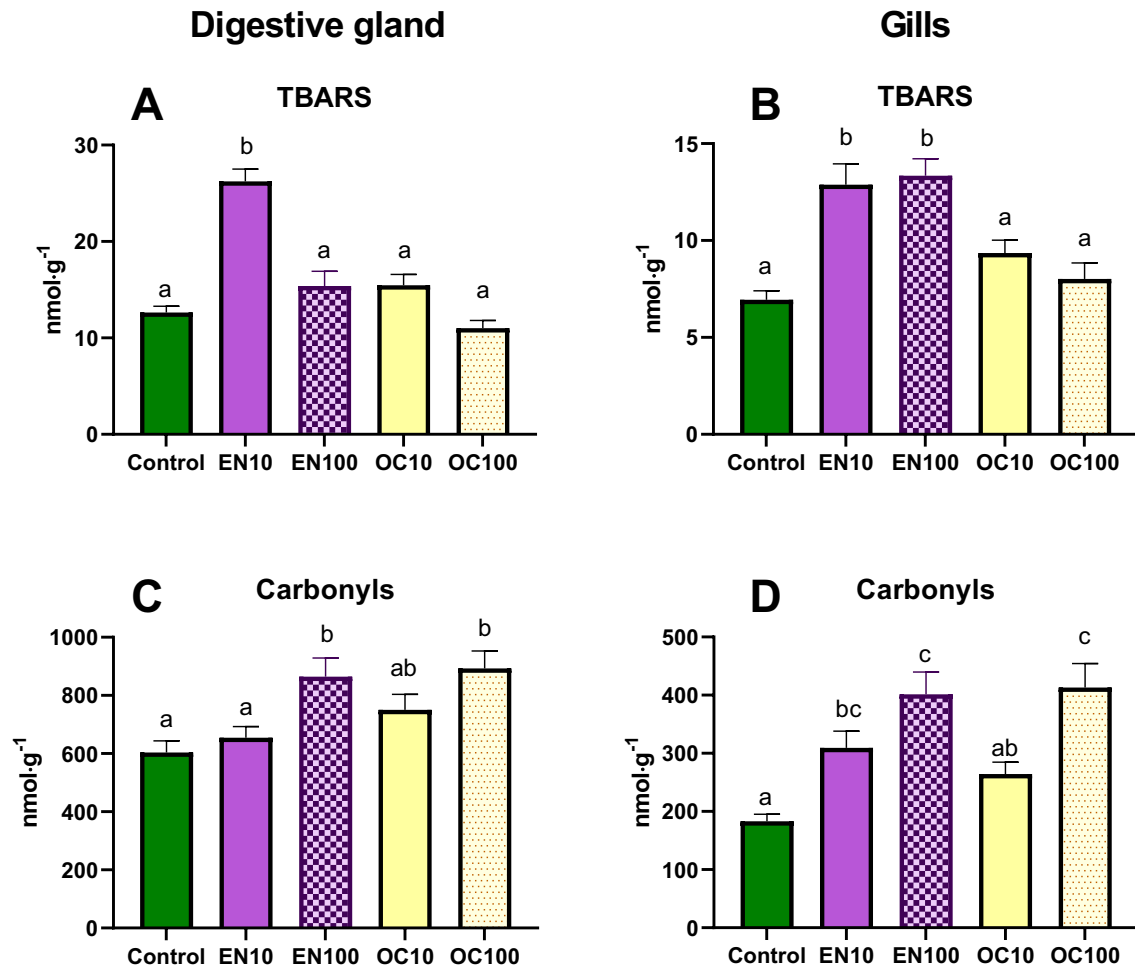

Fig. 2. Effects of ensulizole (EN) and octocrylene (OC) exposures on oxidative stress markers in the digestive gland (A, C) and the gill (B, D) of *M. edulis*. Mussels were exposed for two weeks to $10\ \mu g\ l^{-1}$ (EN10, OC10) or $100\ \mu g\ l^{-1}$ (EN100, OC100) of the respective UV filters. A, B – concentrations of lipid peroxidation products (TBARS), C, D – concentrations of protein carbonyls. Columns that do not share letters represent significantly different values ($P < 0.05$).

to 10 and 100 µg l^{-1} octocrylene had no effect on the tissue TBARS levels in *M. edulis* (Fig. 2A, B). The levels of the protein carbonyls increased in response to the ensulizole exposures (at 100 µg l^{-1} EN only in the digestive gland and at both studied concentrations in the gills) as well as in the digestive gland and the gills of *M. edulis* exposed to 100 µg l^{-1} octocrylene (Fig. 2C, D).

3.4. Detoxification and glutathione metabolism

The activity of a Phase I biotransformation enzyme CPR was not affected at the low ensulizole concentration (10 µg l^{-1}) but was suppressed at 100 µg l^{-1} ensulizole (Fig. 3A). The activities of two

other studied Phase I biotransformation enzymes, EROD and CE, were suppressed by 10 µg l^{-1} ensulizole and stimulated by 100 µg l^{-1} ensulizole in the digestive gland (Fig. 3C, E). The activities of the CPR, EROD and CE in the mussels' gills was not affected by ensulizole exposures except for a modest but statistically significant increase of CE in the high (100 µg l^{-1}) exposure concentration (Fig. 3B, D, F).

Exposure to 10 µg l^{-1} octocrylene suppressed the activity of CPR (by ~1.5-fold) but did not affect the activities of EROD or CE in the digestive gland of the mussels (Fig. 3A, C, E). Exposure to 100 µg l^{-1} octocrylene stimulated the CPR and CE activities (by ~1.2 and 17.2-fold, respectively) and suppressed the EROD activity by ~1.6-fold in
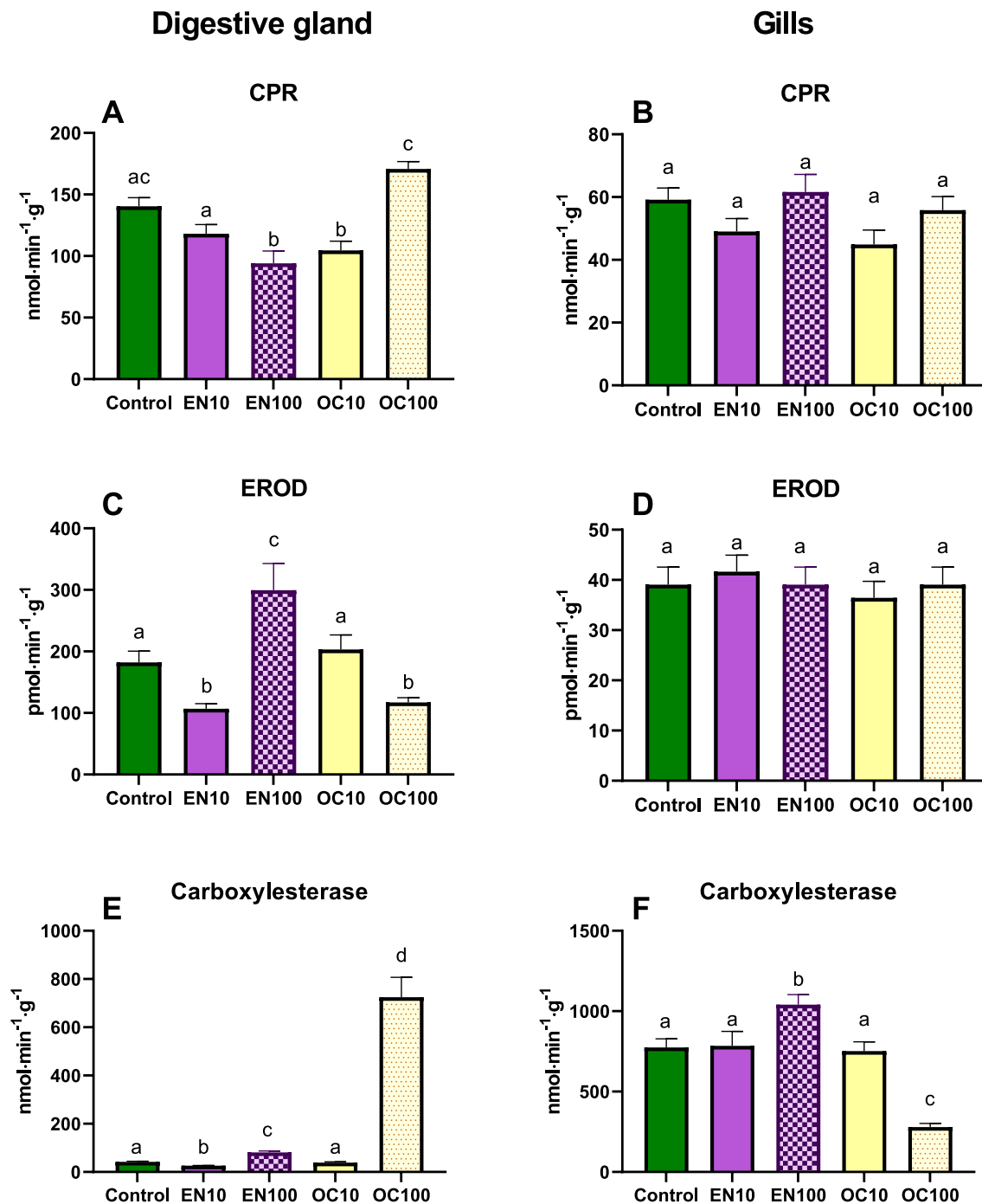

Fig. 3. Effects of ensulizole (EN) and octocrylene (OC) exposures on activities of xenobiotic biotransformation enzymes in the digestive gland (A, C, E) and the gill (B, D, F) of *M. edulis*. Mussels were exposed for two weeks to 10 µg l^{-1} (EN10, OC10) or 100 µg l^{-1} (EN100, OC100) of the respective UV filters. A, B – NADPH–P450 reductase (CPR), C, D - 7-ethoxyresorufin-O-deethylase (EROD), E, F – carboxylesterase activities. Columns that do not share letters represent significantly different values (P < 0.05).
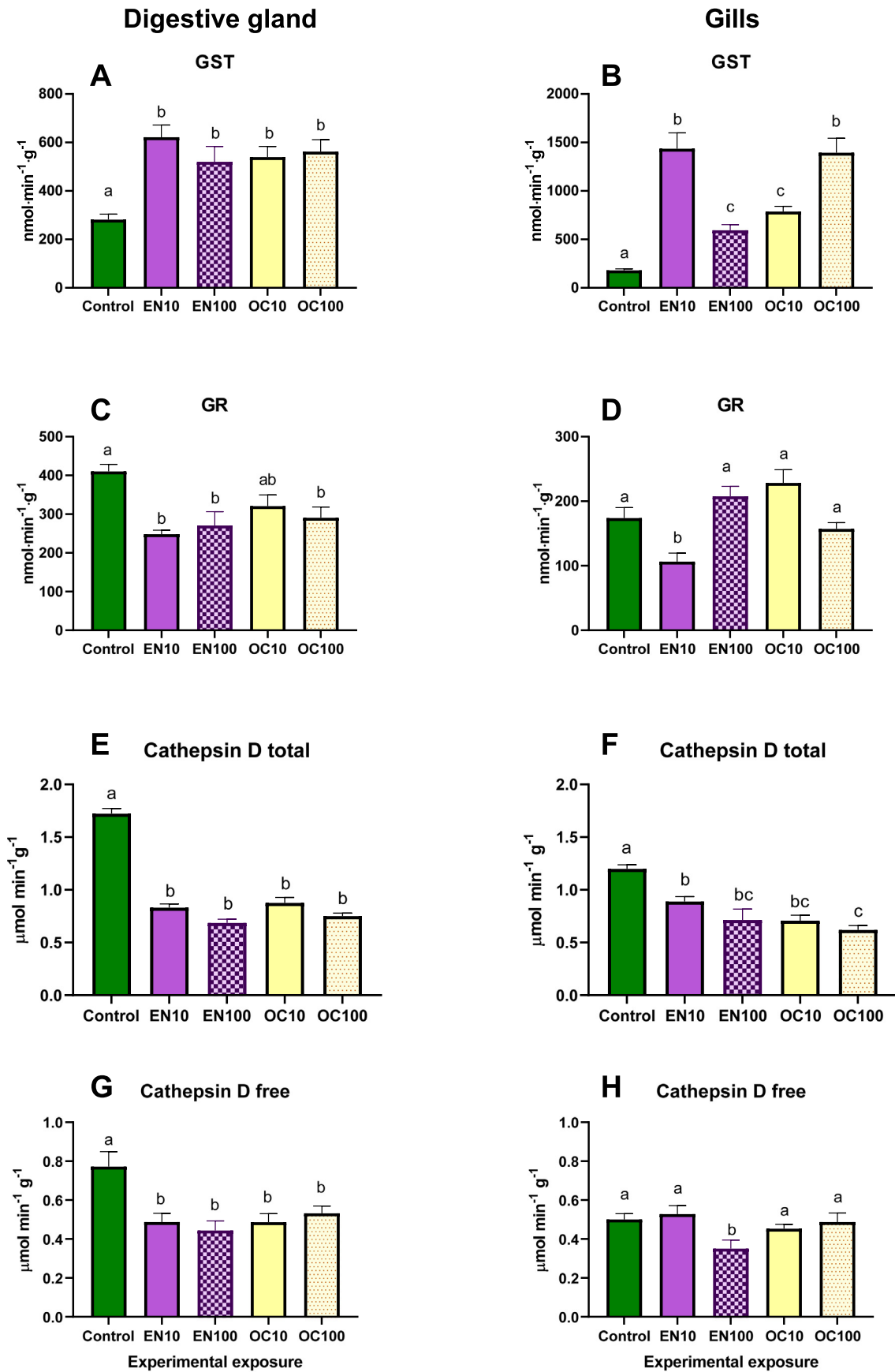
Fig. 4. Effects of ensulizole (EN) and octocrylene (OC) exposures on activities of glutathione-S-transferase (A, B), glutathione reductase (C, D) and cathepsin D (*E*-H) in the digestive gland (A, C, E, G) and the gill (B, D, F, H) of *M. edulis*. Mussels were exposed for two weeks to 10 μg l^{-1} (EN10, OC10) or 100 μg l^{-1} (EN100, OC100) of the respective UV filters. Columns that do not share letters represent significantly different values (*P* < 0.05).

the digestive gland (Fig. 3A, C). Exposure to octocrylene had no effect on the activities of CPR and EROD in the mussel gills (Fig. 3B, D), whereas the CE activity in the gills was suppressed by ~2.8-fold by the high (100 μg l^{-1}) octocrylene concentration (Fig. 3F).

Activity of a Phase II biotransformation enzyme, GST, was stimulated by exposures to 10 and 100 μg l^{-1} of the studied UV filters in the digestive gland and the gills of *M. edulis* (Fig. 4A, B). Activity of the glutathione reductase (GR) was suppressed in the digestive gland (at 10 and μg l^{-1}) and the gills (at 10 μg l^{-1}) of ensulizole-exposed mussels (Fig. 4C, D). Exposure to 100 μg l^{-1} octocrylene suppressed GR activity in the digestive gland (but not the gills) whereas 10 μg l^{-1} octocrylene had no effect (Fig. 4C, D).
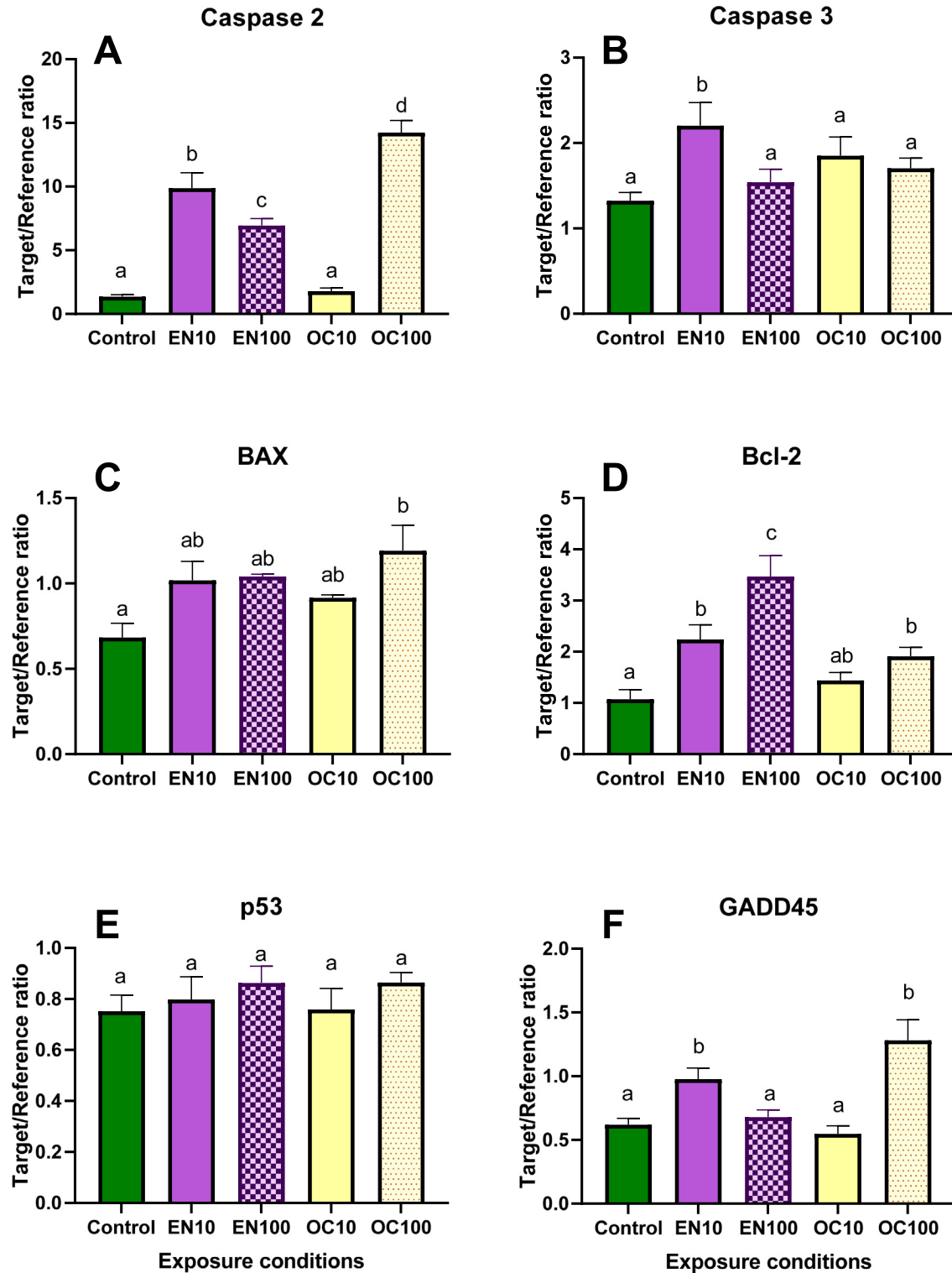

Fig. 5. Effects of ensulizole (EN) and octocrylene (OC) exposures on mRNA expression of apoptotic and DNA damage and repair markers in the digestive gland (A, C, E) and the gill (B, D, F) of *M. edulis*. Mussels were exposed for two weeks to 10 μg l^{-1} (EN10, OC10) or 100 μg l^{-1} (EN100, OC100) of the respective UV filters. Columns that do not share the letters represent significantly different values (P < 0.05).

3.5. Cathepsin D activity

Exposure to ensulizole or octocrylene (10 and 100 μg l^{-1}) led to a significant suppression of the total cathepsin D activity in the digestive gland and gill of the mussels (Fig. 4E, F). Activity of free cathepsin D also decreased in the digestive gland (but not in the gill) of the ensulizole- and octocrylene-exposed mussels (Fig. 4G, H). However, the percent of free cathepsin D increased during exposures to ensulizole and octocrylene in both studied tissues. Thus, in the digestive gland the fraction of free cathepsin D increased from 45% in the control mussels to 55–70% in those exposed to the UV filters. In the gill, the fraction of the free cathepsin D increased from 42% in the control to 50–77% in the mussels exposed to the UV filters.

3.6. Apoptotic markers

Exposure to the low levels of ensulizole (10 μg l^{-1}) led to the elevated expression of caspases 2 and 3 in the digestive gland of the mussels by ~7.3 and 1.7-fold, respectively (Fig. 5A, B). Exposure to 100 μg l^{-1} ensulizole led to a ~ 5.1-fold increase in the caspase 2 mRNA expression but did not affect the transcript levels of caspase 3 (Fig. 5A, B). Exposure to ensulizole did not affect the mRNA levels of BAX but increased the transcript levels of Bcl-2 by ~2.1 and 3.2-fold (at 10 and 100 μg l^{-1} ensulizole, respectively) (Fig. 5C, D).

Exposure to 100 μg l^{-1} octocrylene (but not 10 μg l^{-1}) upregulated the transcript levels of caspase 2, BAX and Bcl-2 by ~10.5, 1.8 and 1.8-fold, respectively (Fig. 5 A, C, D). Expression of caspase 3 mRNA was not

affected by octocrylene exposure regardless of the tested concentration (Fig. 5B).

3.7. DNA damage and repair markers

Exposure to ensulizole or octocrylene had no effect of the mRNA level of the tumor protein p53 in the digestive gland of the mussels (Fig. 5E). Expression of GADD45 mRNA was modestly upregulated by the exposure to 10 μg l^{-1} ensulizole (~1.6-fold) and 100 μg l^{-1} octocrylene (~2.1-fold) but not affected by other experimental exposures (Fig. 5F).

3.8. Inflammatory markers

Transcript levels of inflammatory markers were elevated in the digestive gland of ensulizole-exposed mussels including ~1.5-fold increase in NF-κB mRNA, at both studied ensulizole concentrations, whereas was ~2.4–7.7-fold increase in IL-17 mRNA and ~ 1.4–1.7-fold in COX-2 mRNA (Fig. 6A-C). Exposure to octocrylene had little effect on the mRNA expression of the studied inflammation markers NF-κB, IL-17 or COX-2 except for a ~ 3.9-fold upregulation of IL-17 in the digestive gland of the mussels exposed to 100 μg l^{-1} octocrylene (Fig. 6A, B, C).

3.9. Lipid metabolism marker

Transcript levels of ACC were suppressed in the digestive gland of the mussels exposed to the two studied UV filters (Fig. 6D). Thus, exposure to 10 μg l^{-1} (but not 100 μg l^{-1}) ensulizole led to a ~ 2.1-fold
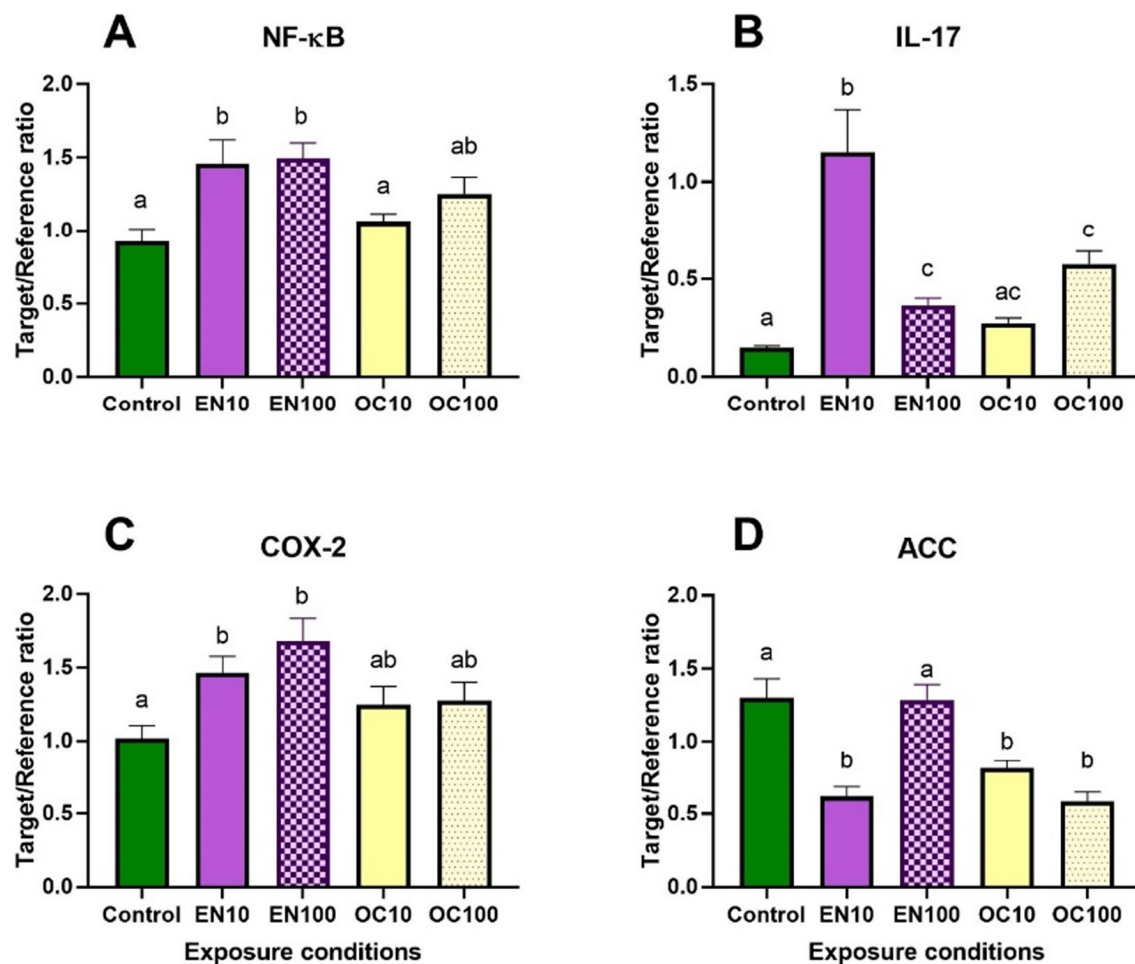

Fig. 6. Effects of ensulizole (EN) and octocrylene (OC) exposures on mRNA expression of inflammation and lipid metabolism markers in the digestive gland (A, C) and the gill (B, D) of *M. edulis*. Mussels were exposed for two weeks to 10 μg l^{-1} (EN10, OC10) or 100 μg l^{-1} (EN100, OC100) of the respective UV filters. Columns that do not share the letters represent significantly different values (P < 0.05).

decrease in ACC mRNA (Fig. 6D). Exposure to octocrylene suppressed the transcript levels of ACC in the digestive gland by ~1.6 and 2.2-fold at 10 and 100 μg l^{-1} octocrylene, respectively (Fig. 6D).

3.10. Biomarker integration: the digestive gland

The multivariate principal component analysis (PCA) using the biochemical and molecular biomarkers identified two principal components (PCs) explaining 54% of variability. The 1st PC (35% of variance) separated the control groups from those exposed to the low concentrations (10 μg l^{-1}) of ensulizole and octocrylene (Fig. 7A). This axis reflected the cellular stress response and was associated with high loadings of cathepsin D, GST and GR activity and mRNA expression of BAX, NF-κB, IL-17, GADD45 and caspase 2 (Fig. 7B, Supplementary Table 1). The 2nd PC (19% variance) separated the groups exposed to high concentrations (100 μg l^{-1}) of ensulizole and octocrylene from all other experimental treatments (Fig. 7A). PC2 can be described as a detoxification-related axis associated with the high loadings of CPR, EROD and CE activities (Fig. 7B, Supplementary Table 1). Notably, the groups exposed to 100 μg l^{-1} of ensulizole and octocrylene were located in two different quadrants of the PCA biplot reflecting different responses of detoxification mechanisms to ensulizole (stimulation of EROD) and octocrylene (stimulation of CPR and CE) (Fig. 7A, B).

The discriminant analysis of the biomarker profiles in the digestive gland of the mussels identified the activities of total cathepsin, CPR, CE and the mRNA expression of GADD45, COX-2 and caspase 2 as significant contributors to the discriminant function (Supplementary Table 2). Based on the discriminant analysis, the biomarker profile of the digestive gland of the mussels exposed to 100 μg l^{-1} octocrylene was most strongly separated from all other treatment groups (Mahalanobis distance D > 2000) (Fig. 7C). The biomarker profiles of the mussels exposed to 10 and 100 μg l^{-1} ensulizole, and to 10 μg l^{-1} octocrylene were close to each other and less well separated from the controls (D = 125–609) (Fig. 7C).

3.11. Biomarker integration: the hemocytes and gill

PCA analysis of the biomarker profiles in the hemocytes and gill of the mussels exposed to different concentrations of the studied UV filters identified two PCs jointly explaining 50% of the biomarker variation (Supplementary Table 3). The 1st PC (30% of variance, "oxidative stress axis") separated the control group from the UV-filters exposed groups and had high loadings of protein carbonyl levels, ROS, NRR, and total cathepsin activity (Fig. 7D, E). The 2nd PC (20% of variance, "glutathione axis") had high loadings of GR and GST activity (Fig. 7B). The groups exposed to 10 or 100 μg l^{-1} of the studied UV filters were not well separated in the plane of the two 1st PCs (Fig. 7D).

The discriminant analysis on the biomarkers in the hemocytes and gills showed that NRR, TBARS levels and activities of GST and CE significantly contribute to the discriminant function (Supplementary Table 4), albeit the biomarker profiles from different treatments were not well separated (Mahalanobis distance D^2 = 48–99) (Fig. 7F). This reflects smaller number of the tested markers as well as weaker biomarker responses in the gill compared to the digestive gland.

4. Discussion

Our present study demonstrates that long-term (14 days) exposure to 10–100 μg l^{-1} of ensulizole or octocrylene does not result in elevated mortality of the blue mussels M. edulis. Earlier studies also report high concentration thresholds for octocrylene lethality (to the best of our knowledge, lethal toxicity of ensulizole has not been tested in aquatic organisms). Thus, in a freshwater crustacean Daphnia magna, immobilization was induced by the concentrations of octocrylene several orders of magnitude higher than typical environmental concentrations (EC$_{50}$ = 3.18 mg l^{-1}) (Park et al., 2017). High thresholds for octocrylene lethality

(LC$_{50}$ = 3.6 mg l^{-1}) were reported in another strain of D. magna, although the threshold for immobilization was considerably lower (EC$_{50}$ = 30 μg l^{-1}) in this strain (Boyd et al., 2021). Interestingly, delayed mortality was observed in D. magna after seven days of exposure to 7.5 μg l^{-1} of octocrylene indicating that some deleterious effects of this UV filter might not be immediately observable in short-term acute studies (Boyd et al., 2021). In zebrafish D. rerio, no mortality was observed in exposures to 69–925 μg l^{-1} (embryos) or to 22–383 μg l^{-1} (adults) of octocrylene (Blüthgen et al., 2014). In marine invertebrate larvae, the reported LC$_{50}$ values for octocrylene were > 650 μg l^{-1} in the blue mussels Mytilus galloprovincialis and 567–1091 μg l^{-1} in the sea urchin Paracentrotus lividus (Giraldo et al., 2017). Taken together, data from our present study and earlier published research indicate that octocrylene and ensulizole are unlikely to cause acute lethal effects in the environmentally relevant concentration range in aquatic organisms. Nevertheless, marked sublethal toxicity of ensulizole and octocrylene in M. edulis indicate the potential negative effects of these UV filters on the mussels from the coastal waters with high environmental loads of sunscreens.

4.1. Bioaccumulation of the UV filters

Our study showed that octocrylene (but not ensulizole) bioaccumulates in the mussels' tissues indicated by an increase in the tissue load of octocrylene in the mussels. High bioconcentration factors (BCF) were reported for octocrylene in aquatic organisms such as the zebrafish Danio rerio (BCF 41–918 depending on the exposure concentration) (Blüthgen et al., 2014; Pawlowski et al., 2019). A rapid decrease in the waterborne concentrations of octocrylene (by >80% within 48 h) has been found in experimental studies with marine algae, as well as embryos and larvae of marine invertebrates and was attributed to the uptake of this lipophilic compound by the organisms (Giraldo et al., 2017). Unlike octocrylene, the concentrations of ensulizole in the exposure water remained stable throughout exposures and no ensulizole accumulation was detected in the mussels' tissue in our present study. Nevertheless, the analysis of biomarkers shows that both ensulizole and octocrylene exposure elicit biological response in the mussels. Sublethal toxicity of ensulizole despite the lack of bioaccumulation in the mussels might reflect active efflux of this compound (that would prevent its accumulation but not interaction with intracellular components) or biotransformation into metabolites undetectable by the analytical method for the parent compound. Strong biological effects in the absence of tissue accumulation have been previously reported for other contaminants. Thus, a pharmaceutical atorvastatin is quickly metabolized in the mussel tissues and shows strong biological effects despite the lack of accumulation of the parent compound (Falfushynska et al., 2019). Furthermore, some essential metals such as Cu and Zn (regulated through the biological efflux mechanisms) may exert toxic effects without notable accumulation in the tissue (Götze et al., 2014; Noor et al., 2021; Wu et al., 2021). The mechanisms that prevent ensulizole accumulation in the mussels are presently not known and require further investigation. However, regardless of these mechanisms, our study shows that the level of bioaccumulation is not a good predictor of toxicity of the studied organic UV filters in M. edulis.

4.2. Effects of ensulizole and octocrylene on xenobiotic detoxification mechanisms

Activity of the Phase I biotransformation enzymes CPR and CYP450 1A were markedly higher in the digestive gland than in the gills of M. edulis, consistent with the role of the digestive gland as a main site of xenobiotic biotransformation in bivalves (Livingstone, 1998). Exposures to ensulizole and octocrylene modulated the activity of xenobiotic detoxification enzymes in the digestive gland of M. edulis, whereas in the gill no change (CPR and CYP450 1A) or modest alterations (carboxylesterase) were found. Low concentrations (10 μg l^{-1}) of ensulizole suppressed the activity of all three studied Phase I

Fig. 7. PCA score plots (A, D), variable loading plots (B, E) and discriminant analysis plots (C, F) based on the studied biomarkers from *M. edulis* exposed to ensulizole and octocrylene. A, D – p[...] experimental group in the coordinate plane of 1st two principal components. B, E – variable loading plots showing how much weight different biomarkers have on each of the two 1st principal[...] samples from different experimental groups in the plane of two main roots of discriminant analysis. Numbers correspond to Mahalanobis distances between group centroids. Experimental groups[...] – 100 µg l⁻¹ ensulizole; OLC – 10 µg l⁻¹ octocrylene; OHC – 100 µg l⁻¹ octocrylene.

Gills
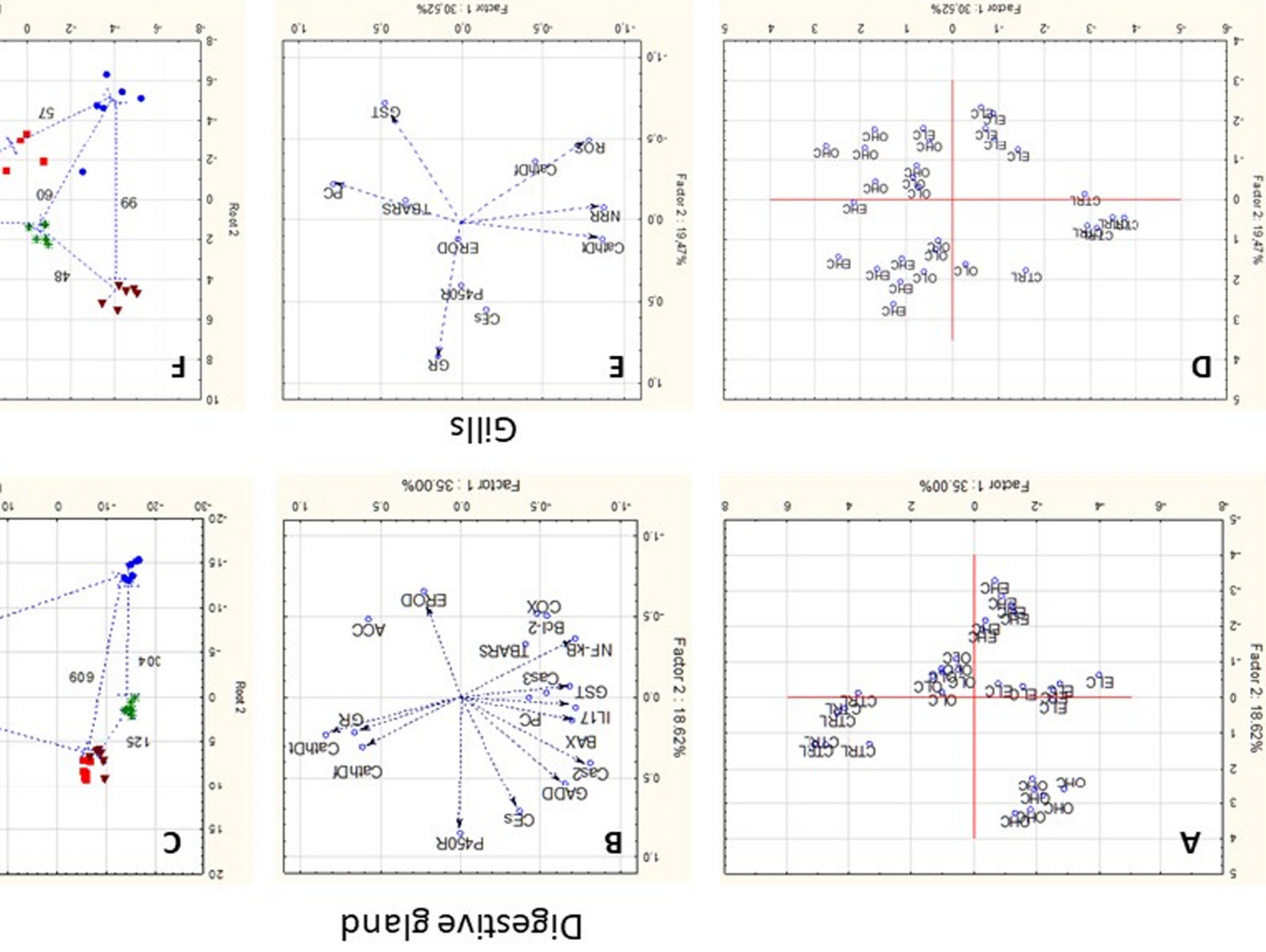
Digestive gland

detoxification enzymes in the mussels' digestive gland. Notably, in the mussels exposed to the high concentration ($100 \ \mu g \ l^{-1}$) of ensulizole, the digestive gland CPR activity was further suppressed whereas activities of CYP450 1A and carboxylesterase increased above the baseline levels. Similar to ensulizole, effects of octocrylene on CPR and carboxylesterase activity showed a non-linear concentration response with a suppression by the low ($10 \ \mu g \ l^{-1}$) and stimulation by the high concentrations ($100 \ \mu g \ l^{-1}$). In contrast, CYP450 1A was suppressed by the high concentration of octocrylene. Earlier studies in freshwater insect larvae, *Chironomus riparius* showed that short-term (96 h) exposure to $1 \ mg \ l^{-1}$ of octocrylene suppressed transcription of a Phase I enzyme Cyp6b7 whereas three other tested CYP450 enzymes (Cyp4d2, Cyp9f2 and Cyp12a2) were not affected (Muñiz-González and Martínez-Guitarte, 2020). Suppression of the Phase I enzyme activities by low environmentally relevant concentrations ($10 \ \mu g \ l^{-1}$) of ensulizole and octocrylene might decrease the mussels' ability to detoxify organic pollutants and increase sensitivity to contaminants.

Unlike Phase I enzymes, activity of a Phase II biotransformation enzyme GST was consistently stimulated by exposure to ensulizole and octocrylene in the digestive gland and the gills of *M. edulis*. Notably, the activity of glutathione reductase (GR), an enzyme involved in glutathione recycling, was suppressed in the mussels exposed to the studied UV filters. Similarly, an increase in the GST and suppression of the GR activity has been reported in fish exposed to waterborne ensulizole (Campos et al., 2017; Grabicova et al., 2013). The suppression of the GR activity might limit the amount of reduced glutathione that serves as an essential co-substrate for GST and could therefore counteract the observed increase in the GST activity (Csiszár et al., 2016). Overall, exposure to ensulizole and octocrylene might dysregulate the xenobiotic biotransformation system of the mussels due to the opposing effects of these compounds on Phase I and Phase II biotransformation enzymes. This notion is supported by the multivariate analyses showing different vector directions for xenobiotic biotransformation markers (Fig. 7). Further studies are needed to determine whether this dysregulation translates into the lower capacity for xenobiotic biotransformation and results in chemosensitization of the mussels exposed to UV filters.

4.3. Effects of ensulizole and octocrylene on cellular stress responses

Exposure to ensulizole and octocrylene induced oxidative stress indicated by accumulation of oxidative lesions (lipid peroxidation products and protein carbonyls) in the gills and digestive gland of the mussels as well as increase in the ROS levels in hemocytes. Generally, ensulizole appeared a stronger pro-oxidant than octocrylene, especially at the low ($10 \ \mu g \ l^{-1}$) environmentally relevant concentration. In octocrylene-exposed mussels, there was no increase in TBARS levels, and accumulation of protein carbonyls was observed only at the high ($100 \ \mu g \ l^{-1}$) octocrylene concentration. The oxidative stress responses to ensulizole appear especially strong in the gill, which is the first organ coming in contact with this hydrophilic contaminant during waterborne exposures. For the lipophilic octocrylene, the degree of oxidative stress responses are comparable in the gill and the digestive gland. The pro-oxidant effects of the UV filters have not been extensively studied in aquatic organisms but available data are consistent with the notion of the oxidative stress involvement in the toxicity of ensulizole and, to a lesser degree, octocrylene. Thus, in the rainbow trout, *Oncorhynchus mykiss*, long-term (42 days) exposure to $1 \ mg \ l^{-1}$ ensulizole led to a significant decrease of activity of glutathione reductase (GR) indicating suppression of glutathione-dependent antioxidant defense (Grabicova et al., 2013). Activities of two other key antioxidant enzymes, superoxide dismutase (SOD) and catalase (CAT) were not affected by ensulizole exposure in the trout (Grabicova et al., 2013). In zebrafish *Danio rerio* 14 days of exposure to $0.5–5 \ mg \ l^{-1}$ ensulizole led to accumulation of lipid peroxidation products (Huang et al., 2020). In contrast, exposure to octocrylene in the sediments ($0.23–18.23 \ mg \ kg^{-1}$) had no effect on the lipid peroxidation or activity

of antioxidant enzymes (catalase) in the midge larvae *C. riparius* (Campos et al., 2017).

Inflammation and apoptosis are common responses to exposures to environmental stressors (including toxicants) that induce oxidative stress and damage to the lipids, proteins or DNA (Orrenius et al., 2011). Molecular (mRNA) markers indicated that exposure to ensulizole and octocrylene induced inflammation, apoptosis and autophagy in the digestive gland of the mussels. Similar to the pro-oxidant action of the two studied UV filters, ensulizole appears to have a stronger pro-inflammatory and pro-apoptotic effect than octocrylene in *M. edulis*. Thus, in ensulizole-exposed mussels, all three studied inflammatory markers (NF-κB, COX-2 and IL-17) were transcriptionally upregulated during exposures to both experimental concentrations (10 and $100 \ \mu g \ l^{-1}$). In contrast, octocrylene induced a mild elevation of IL-17 mRNA levels only at the high ($100 \ \mu g \ l^{-1}$) exposure concentration, whereas the transcript levels of NF-κB and COX-2 did not respond to octocrylene exposures. Likewise, the upregulation of apoptotic pathways was more pronounced in ensulizole-exposed mussels compared with their octocrylene-exposed counterparts. Thus, exposure to both 10 and $100 \ \mu g \ l^{-1}$ of ensulizole led to a strong increase in mRNA expression of a stress-induced caspase 2 implicated in the response to oxidative stress and DNA damage (Fava et al., 2012; Miles et al., 2017). In octocrylene-exposed mussels, only $100 \ \mu g \ l^{-1}$ exposure led to an increase in caspase 2 mRNA. Exposure to low concentrations of ensulizole also increased the transcript levels of an executioner caspase 3 involved in the cleavage of cellular proteins (Shalini et al., 2015). Unlike ensulizole, octocrylene had no effect on caspase 3 expression in the mussels. Notably, transcript levels of an anti-apoptotic protein Bcl-2 and a key DNA repair regulator GADD45 were upregulated in the digestive gland of the mussels exposed to $10–100 \ \mu g \ l^{-1}$ ensulizole or to $100 \ \mu g \ l^{-1}$ octocrylene. However, this upregulation was insufficient to prevent apoptosis as shown by the transcriptional induction of caspases 2 and 3.

Lipid metabolism has been recently identified as an important target for toxicity in lipophilic UV filters such as octocrylene (Blüthgen et al., 2014; Stien et al., 2019; Stien et al., 2020). Thus, in corals (*Pocillopora damicornis*) exposure to $5–1000 \ \mu g \ l^{-1}$ octocrylene led to a strong accumulation of acylcarnitines indicating disturbances of fatty acid metabolism and β-oxidation (Stien et al., 2019). Furthermore, steroid metabolism was negatively affected by exposures to $50 \ \mu g \ l^{-1}$ of octocrylene in the corals (Stien et al., 2020). Alterations of lipid metabolism were shown by the transcriptomic shifts in the respective pathways induced by the octocrylene exposure ($383 \ \mu g \ l^{-1}$) in zebrafish (Blüthgen et al., 2014). Our present study indicates that ensulizole and octocrylene might also interfere with the lipid metabolism in the mussels *M. edulis*. Thus, mRNA expression of a key enzyme regulating the fatty acid biosynthesis, acetyl-CoA carboxylase (ACC) was suppressed by low concentration of ensulizole and by both studied concentrations of octocrylene. However, transcript levels of the peroxisome proliferator-activated receptor gamma (PPAR-γ) that controls accumulation, uptake and storage of fatty acids (Varga et al., 2011) were not affected by the studied UV filters in *M. edulis*. Disturbances of the fatty acid metabolism caused by the UV filters might contribute to the observed inflammatory responses during UV filter exposures due to the tight link between the lipid metabolism and inflammation (Varga et al., 2011). However, the available limited data do not allow establishing the cause-effect relationships between the fatty acid dysregulation and the cellular stress (including inflammation and apoptosis) during exposures to the UV filters in aquatic organisms, and this aspect of the UV filter toxicity warrants further investigation.

4.4. Conclusions and outlook

Our data demonstrate that two common UV filters, ensulizole and octocrylene, induce sublethal toxic effects in the blue mussels *M. edulis*, despite the lack of acute toxicity at the environmentally

relevant concentrations. Based on the integrated multi-biomarker assessment, these sublethal toxic effects involve dysregulation of xenobiotic biotransformation system, oxidative stress, DNA damage, inflammation and apoptosis. Notably, unlike octocrylene that induced stress responses in the concentration-dependent manner, ensulizole exposures appeared more toxic at the low ($10\ \mu g\ l^{-1}$) levels than at the high ($100\ \mu g\ l^{-1}$) experimental concentration. The reasons for this non-linear concentration response are presently not known but might reflect the suppression of the cellular detoxification system by the lower ($10\ \mu g\ l^{-1}$) ensulizole concentration which was partially or fully reversed during exposure to higher ensulizole levels. These findings emphasize the importance of including low concentrations of UV filters in environmental toxicity testing and demonstrate the need for further studies with higher resolution of experimental test concentrations. Furthermore, our data show that bioaccumulation and/or lipophilicity of the UV filter is not a good predictor of its toxic effects in marine organisms such as mussels. The sublethal toxicity assessed by the oxidative lesions, apoptosis or inflammation markers was stronger in a hydrophilic UV filter ensulizole (despite its lack of accumulation in the mussel tissues) than in a strongly hydrophobic and bioaccumulating octocrylene. These data indicate that toxic effects of emerging organic pollutants such as UV filters might not be easily predicted based on physico-chemical considerations and emphasize the importance of conducting bioassays for detecting toxicity and elucidating the toxic mechanisms of emerging pollutants in coastal marine ecosystems.

CRediT authorship contribution statement

Halina Falfushynska: Conceptualization, Methodology, Validation, Investigation, Data curation, Formal analysis, Visualization, Writing – review & editing. **Eugene P. Sokolov:** Methodology, Validation, Data curation, Investigation, Writing – review & editing. **Kathrin Fisch:** Methodology, Validation, Supervision, Writing – review & editing. **Hatem Gazie:** Methodology, Validation. **Detlef E. Schulz-Bull:** Resources, Supervision. **Inna M. Sokolova:** Conceptualization, Formal analysis, Visualization, Funding acquisition, Project administration, Writing – original draft, Writing – review & editing.

Declaration of competing interest

The authors declare that they have no known competing financial interests or personal relationships that could have appeared to influence the work reported in this paper.

Acknowledgements

Appendix A. Supplementary data

Supplementary data to this article can be found online at https://doi.org/10.1016/j.scitotenv.2021.149171.

References

Apel, C., Joerss, H., Ebinghaus, R., 2018. Environmental occurrence and hazard of organic UV stabilizers and UV filters in the sediment of European North and Baltic seas. Chemosphere 212, 254–261.

Bachelot, M., Li, Z., Munaron, D., Le Gall, P., Casellas, C., Fenet, H., Gomez, E., 2012. Organic UV filter concentrations in marine mussels from French coastal regions. Sci. Total Environ. 420, 273–279.

Balázs, A., Krifaton, C., Orosz, I., Szoboszlay, S., Kovács, R., Csenki, Z., Urbányi, B., Kriszt, B., 2016. Hormonal activity, cytotoxicity and developmental toxicity of UV filters. Ecotoxicol. Environ. Saf. 131, 45–53.

Balk, L., Meijer, J., Bergstrand, A., Aström, A., Morgenstern, R., Seidegård, J., DePierre, J.W., 1982. Preparation and characterization of subcellular fractions from the liver of the northern pike, Esox lucius. Biochem. Pharmacol. 31, 1491–1500.

Blasco, J., Trombini, C., Sendra, M., Araujo, C.V.M., 2020. Environmental risk assessment of sunscreens. In: Sánchez-Quiles, A. Tovar-Sánchez D., Blasco, J. (Eds.), Sunscreens in Coastal Ecosystems: Occurrence, Behavior, Effect and Risk. Springer International Publishing, Cham, pp. 163–184.

Blüthgen, N., Meili, N., Chew, G., Odermatt, A., Fent, K., 2014. Accumulation and effects of the UV-filter octocrylene in adult and embryonic zebrafish (Danio rerio). Sci. Total Environ. 476–477, 207–217.

Boyd, A., Stewart, C.B., Philibert, D.A., How, Z.T., El-Din, M.G., Tierney, K.B., Blewett, T.A., 2021. A burning issue: the effect of organic ultraviolet filter exposure on the behaviour and physiology of Daphnia magna. Sci. Total Environ. 750, 141707.

Campos, D., Gravato, C., Quintaneiro, C., Golovko, O., Žlábek, V., Soares, A.M.V.M., Pestana, J.L.T., 2017. Toxicity of organic UV-filters to the aquatic midge Chironomus riparius. Ecotoxicol. Environ. Saf. 143, 210–216.

Carlberg, I., Mannervik, B., 1975. Purification and characterization of the flavoenzyme glutathione reductase from rat liver. J. Biol. Chem. 250, 5475–5480.

Corinaldesi, C., Marcellini, F., Nepote, E., Damiani, E., Danovaro, R., 2018. Impact of inorganic UV filters contained in sunscreen products on tropical stony corals (Acropora spp.). Sci. Total Environ. 637–638, 1279–1285.

Csiszár, J., Horváth, E., Bela, K., Galle, A., 2016. Glutathione-Related Enzyme System: Glutathione Reductase (GR), Glutathione Transferases (GSTs) and Glutathione Peroxidases (GPXs), pp. 137–158.

Downs, C.A., Kramarsky-Winter, E., Segal, R., Fauth, J., Knutson, S., Bronstein, O., Ciner, F.R., Jeger, R., Lichtenfeld, Y., Woodley, C.M., et al., 2016. Toxicopathological effects of the sunscreen UV filter, oxybenzone (Benzophenone-3), on coral planulae and cultured primary cells and its environmental contamination in Hawaii and the U.S. Virgin Islands. Arch. Environ. Contam. Toxicol. 70, 265–288.

Faggio, C., Tsarpali, V., Dailianis, S., 2018. Mussel digestive gland as a model tissue for assessing xenobiotics: an overview. Sci. Total Environ. 636.

Falfushynska, H., Sokolov, E.P., Haider, F., Oppermann, C., Kragl, U., Ruth, W., Stock, M., Glufke, S., Winkel, E.J., Sokolova, I.M., 2019. Effects of a common pharmaceutical, atorvastatin, on energy metabolism and detoxification mechanisms of a marine bivalve Mytilus edulis. Aquat. Toxicol. 208, 47–61.

Fava, L.L., Bock, F.J., Geley, S., Villunger, A., 2012. Caspase-2 at a glance. J. Cell Sci. 125, 5911–5915.

Fel, J.-P., Lacherez, C., Bensetra, A., Mezzache, S., Béraud, E., Léonard, M., Allemand, D., Ferrier-Pagès, C., 2019. Photochemical response of the scleractinian coral Stylophora pistillata to some sunscreen ingredients. Coral Reefs 38, 109–122.

Fisch, K., Waniek, J.J., Schulz-Bull, D.E., 2017. Occurrence of pharmaceuticals and UV-filters in riverine run-offs and waters of the german Baltic Sea. Mar. Pollut. Bull. 124, 388–399.

Fisch, K., Zhang, R., Zhou, M., Schulz-Bull, D.E., Waniek, J.J., 2021. PPCPs - a human and veterinary fingerprint in the Pearl River delta and northern south China Sea. Emerg. Contam. 7, 10–21.

Gaitán-Espitia, J.D., Quintero-Galvis, J.F., Mesas, A., D'Elía, G., 2016. Mitogenomics of southern hemisphere blue mussels (Bivalvia: Pteriomorphia): insights into the evolutionary characteristics of the Mytilus edulis complex. Sci. Rep. 6, 26853.

Gilbert, E., Pirot, F., Bertholle, V., Roussel, L., Falson, F., Padois, K., 2013. Commonly used UV filter toxicity on biological functions: review of last decade studies. Int. J. Cosmet. Sci. 35, 208–219.

Giraldo, A., Montes, R., Rodil, R., Quintana, J.B., Vidal-Liñán, L., Beiras, R., 2017. Ecotoxicological evaluation of the UV filters ethylhexyl dimethyl p-aminobenzoic acid and octocrylene using marine organisms Isochrysis galbana, Mytilus galloprovincialis and Paracentrotus lividus. Arch. Environ. Contam. Toxicol. 72, 606–611.

Gosling, E., 2003. Morphology of bivalves. Bivalve Molluscs. Blackwell Publishing Ltd., pp. 7–43.

Götze, S., Matoo, O.B., Beniash, E., Saborowski, R., Sokolova, I.M., 2014. Interactive effects of CO2 and trace metals on the proteasome activity and cellular stress response of marine bivalves Crassostrea virginica and Mercenaria mercenaria. Aquat. Toxicol. 149, 65–82.

Grabicova, K., Fedorova, G., Burkina, V., Steinbach, C., Schmidt-Posthaus, H., Zlabek, V., Kocour Kroupova, H., Grabic, R., Randak, T., 2013. Presence of UV filters in surface water and the effects of phenylbenzimidazole sulfonic acid on rainbow trout (Oncorhynchus mykiss) following a chronic toxicity test. Ecotoxicol. Environ. Saf. 96, 41–47.

Guengerich, F.P., Martin, M.V., Sohl, C.D., Cheng, Q., 2009. Measurement of cytochrome P450 and NADPH-cytochrome P450 reductase. Nat. Protoc. 4, 1245–1251.

Habig, W.H., Pabst, M.J., Jakoby, W.B., 1974. Glutathione S-transferases. The first enzymatic step in mercapturic acid formation. J. Biol. Chem. 249, 7130–7139.

He, T., Tsui, M.M.P., Tan, C.J., Ng, K.Y., Guo, F.W., Wang, L.H., Chen, T.H., Fan, T.Y., Lam, P.K.S., Murphy, M.B., 2019. Comparative toxicities of four benzophenone ultraviolet filters to two life stages of two coral species. Sci. Total Environ. 651, 2391–2399.

Hosokawa, M., Satoh, T., 2002. Measurement of carboxylesterase (CES) activities. Curr. Protoc. Toxicol. Chapter 4 (Unit 4.7). https://doi.org/10.1002/0471140856.tx0407s10.

Huang, X., Li, Y., Wang, T., Liu, H., Shi, J., Zhang, X., 2020. Evaluation of the oxidative stress status in zebrafish (Danio rerio) liver induced by three typical organic UV filters (BP-4, PABA and PBSA). Int. J. Environ. Res. Public Health 17.

Kaiser, D., Sieratowicz, A., Zielke, H., Oetken, M., Hollert, H., Oehlmann, J., 2012. Ecotoxicological effect characterisation of widely used organic UV filters. Environ. Pollut. 163, 84–90.

Khlebovich, V.V., 2017. Acclimation of animal organisms: basic theory and applied aspects. Biol. Bull. Rev. 7, 279–286.

Langford, K.H., Thomas, K.V., 2008. Inputs of chemicals from recreational activities into the Norwegian coastal zone. J. Environ. Monit. 10, 894–898.

Livingstone, D.R., 1998. The fate of organic xenobiotics in aquatic ecosystems: quantitative and qualitative differences in biotransformation by invertebrates and fish. Comp. Biochem. Physiol. A Mol. Integr. Physiol. 120, 43–49.

Lozano, C., Givens, J., Stien, D., Matallana-Surget, S., Lebaron, P., 2020. Bioaccumulation and toxicological effects of UV-filters on marine species. In: Sánchez-Quiles, A. Tovar-Sánchez D., Blasco, J. (Eds.), Sunscreens in Coastal Ecosystems: Occurrence, Behavior, Effect and Risk. Springer International Publishing, Cham, pp. 85–130.

Luo, Z., Li, Z., Xie, Z., Sokolova, I.M., Song, L., Peijnenburg, W.J.G.M., Hu, M., Wang, Y., 2020. Rethinking Nano-TiO2 safety: overview of toxic effects in humans and aquatic animals. Small 2002019.

Miles, M.A., Kitevska-Ilioski, T., Hawkins, C.J., 2017. Old and novel functions of Caspase-2. Int. Rev. Cell Mol. Biol. 332, 155–212.

Minetto, D., Volpi Ghirardini, A., Libralato, G., 2016. Saltwater ecotoxicology of Ag, Au, CuO, TiO2, ZnO and C60 engineered nanoparticles: an overview. Environ. Int. 92–93, 189–201.

Mitchelmore, C.L., He, K., Gonsior, M., Hain, E., Heyes, A., Clark, C., Younger, R., Schmitt-Kopplin, P., Feerick, A., Conway, A., et al., 2019. Occurrence and distribution of UV-filters and other anthropogenic contaminants in coastal surface water, sediment, and coral tissue from Hawaii. Sci. Total Environ. 670, 398–410.

Mohammadi Bardbori, A., 2014. Assay for quantitative determination of CYP1A1 enzyme activity using 7-ethoxyresorufin as standard substrate EROD assay. Protoc. Exch. https://doi.org/10.1038/protex.2014.043.

Muñiz-González, A.-B., Martínez-Guitarte, J.-L., 2020. Unveiling complex responses at the molecular level: transcriptional alterations by mixtures of bisphenol a, octocrylene, and 2'-ethylhexyl 4- (dimethylamino)benzoate on Chironomus riparius. Ecotoxicol. Environ. Saf. 206, 111199.

Muñoz, M., Cedeño, R., Rodríguez, J., van der Knaap, W.P.W., Mialhe, E., Bachère, E., 2000. Measurement of reactive oxygen intermediate production in haemocytes of the penaeid shrimp, Penaeus vannamei. Aquaculture 191, 89–107.

Noor, M.N., Wu, F., Sokolov, E.P., Falfushynska, H., Timm, S., Haider, F., Sokolova, I.M., 2021. Salinity-dependent effects of ZnO nanoparticles on bioenergetics and intermediate metabolite homeostasis in a euryhaline marine bivalve, Mytilus edulis. Sci. Total Environ. 774, 145195. https://doi.org/10.1016/j.scitotenv.2021.145195.

Ohkawa, H., Ohishi, N., Yagi, K., 1979. Assay for lipid peroxides in animal tissues by thiobarbituric acid reaction. Anal. Biochem. 95, 351–358.

O'Malley, E., O'Brien, J.W., Tscharke, B., Thomas, K.V., Mueller, J.F., 2019. Per capita loads of organic UV filters in Australian wastewater influent. Sci. Total Environ. 662, 134–140.

Orrenius, S., Nicotera, P., Zhivotovsky, B., 2011. Cell death mechanisms and their implications in toxicology. Toxicol. Sci. 119, 3–19.

Park, C.-B., Jang, J., Kim, S., Kim, Y.J., 2017. Single- and mixture toxicity of three organic UV-filters, ethylhexyl methoxycinnamate, octocrylene, and avobenzone on Daphnia magna. Ecotoxicol. Environ. Saf. 137, 57–63.

Pawlowski, S., Lanzinger, A.C., Dolich, T., Füßl, S., Salinas, E.R., Zok, S., Weiss, B., Hefner, N., Van Sloun, P., Hombeck, H., et al., 2019. Evaluation of the bioaccumulation of octocrylene after dietary and aqueous exposure. Sci. Total Environ. 672, 669–679.

Pfaffl, M.W., 2001. A new mathematical model for relative quantification in real-time RT-PCR. Nucleic Acids Res. 29, 2002–2007.

Pintado-Herrera, M.G., Lara Martín, P.A., 2020. Fate and behavior of UV filters in the marine environment. In: Sánchez-Quiles, A. Tovar-Sánchez D., Blasco, J. (Eds.), Sunscreens in Coastal Ecosystems: Occurrence, Behavior, Effect and Risk. Springer International Publishing, Cham, pp. 59–83.

Qi, P., Huang, H., Guo, B., Liao, Z., Liu, H., Tang, Z., He, Y., 2019. A novel interleukin-1 receptor-associated kinase-4 from thick shell mussel Mytilus coruscus is involved in inflammatory response. Fish Shellfish Immunol. 84, 213–222.

Repetto, G., del Peso, A., Zurita, G., 2008. Neutral red uptake assay for the estimation of cell viability/cytotoxicity. Nat Protoc 3, 1125–1131.

Reznick, A.Z., Packer, L., 1994. Oxidative damage to proteins: spectrophotometric method for carbonyl assay. Methods Enzymol. 357–363.

Rodil, R., Moeder, M., 2008. Development of a method for the determination of UV filters in water samples using stir bar sorptive extraction and thermal desorption–gas chromatography–mass spectrometry. J. Chromatogr. A 1179, 81–88.

Ruszkiewicz, J.A., Pinkas, A., Ferrer, B., Peres, T.V., Tsatsakis, A., Aschner, M., 2017. Neurotoxic effect of active ingredients in sunscreen products, a contemporary review. Toxicol. Rep. 4, 245–259.

Sánchez-Quiles, D., Tovar-Sánchez, A., 2015. Are sunscreens a new environmental risk associated with coastal tourism? Environ. Int. 83, 158–170.

Sang, Z., Leung, K.S.-Y., 2016. Environmental occurrence and ecological risk assessment of organic UV filters in marine organisms from Hong Kong coastal waters. Sci. Total Environ. 566–567, 489–498.

Schneider, S.L., Lim, H.W., 2019. Review of environmental effects of oxybenzone and other sunscreen active ingredients. J. Am. Acad. Dermatol. 80, 266–271.

Scown, T.M., van Aerle, R., Tyler, C.R., 2010. Review: do engineered nanoparticles pose a significant threat to the aquatic environment? Crit. Rev. Toxicol. 40, 653–670.

Shalini, S., Dorstyn, L., Dawar, S., Kumar, S., 2015. Old, new and emerging functions of caspases. Cell Death Differ. 22, 526–539.

Steffen, J.B.M., Falfushynska, H.I., Piontkivska, H., Sokolova, I.M., 2020. Molecular biomarkers of the mitochondrial quality control are differently affected by hypoxia-reoxygenation stress in marine bivalves Crassostrea gigas and Mytilus edulis. Front. Mar. Sci. 7.

Stien, D., Clergeaud, F., Rodrigues, A.M.S., Lebaron, K., Pillot, R., Romans, P., Fagervold, S., Lebaron, P., 2019. Metabolomics reveal that octocrylene accumulates in Pocillopora damicornis tissues as fatty acid conjugates and triggers coral cell mitochondrial dysfunction. Anal. Chem. 91, 990–995.

Stien, D., Suzuki, M., Rodrigues, A.M.S., Yvin, M., Clergeaud, F., Thorel, E., Lebaron, P., 2020. A unique approach to monitor stress in coral exposed to emerging pollutants. Sci. Rep. 10, 9601.

Stuckas, H., Knöbel, L., Schade, H., Breusing, C., Hinrichsen, H.-H., Bartel, M., Langguth, K., Melzner, F., 2017. Combining hydrodynamic modelling with genetics: can passive larval drift shape the genetic structure of Baltic Mytilus populations? Mol. Ecol. 26, 2765–2782.

Tsui, M.M.P., Leung, H.W., Kwan, B.K.Y., Ng, K.-Y., Yamashita, N., Taniyasu, S., Lam, P.K.S., Murphy, M.B., 2015. Occurrence, distribution and ecological risk assessment of multiple classes of UV filters in marine sediments in Hong Kong and Japan. J. Hazard. Mater. 292, 180–187.

Varga, T., Czimmerer, Z., Nagy, L., 2011. PPARs are a unique set of fatty acid regulated transcription factors controlling both lipid metabolism and inflammation. Biochim. Biophys. Acta 1812, 1007–1022.

Varvio, S.L., Koehn, R.K., Väinölä, R., 1988. Evolutionary genetics of the Mytilus edulis complex in the North Atlantic region. Mar. Biol. 98, 51–60.

Wu, F., Sokolov, E.P., Dellwig, O., Sokolova, I.M., 2020. Season-dependent effects of ZnO nanoparticles and elevated temperature on bioenergetics of the blue mussel Mytilus edulis. Chemosphere 263, 127780.

Yan, S., Liang, M., Chen, R., Hong, X., Zha, J., 2020. Reproductive toxicity and estrogen activity in japanese medaka (Oryzias latipes) exposed to environmentally relevant concentrations of octocrylene. Environ. Pollut. 261, 114104.

Yung, M., Mouneyrac, C., Leung, K., 2015. Ecotoxicity of Zinc Oxide Nanoparticles in the Marine Environment, pp. 1–17.

Zhang, Q.Y., Ma, X.Y., Wang, X.C., Ngo, H.H., 2016. Assessment of multiple hormone activities of a UV-filter (octocrylene) in zebrafish (Danio rerio). Chemosphere 159, 433–441.